A hydrogen-bonding triad stabilizes the chemical transition state of a group I ribozyme

Scott A Strobel and Lori Ortoleva-Donnelly

Background: The group I intron is an RNA enzyme capable of efficiently catalyzing phosphoryl-transfer reactions. Functional groups that stabilize the chemical transition state of the cleavage reaction have been identified, but they are all located within either the 5′-exon (P1) helix or the guanosine cofactor, which are the substrates of the reaction. Functional groups within the ribozyme active site are also expected to assist in transition-state stabilization, and their role must be explored to understand the chemical basis of group I intron catalysis.

Results: Using nucleotide analog interference mapping and site-specific functional group substitution experiments, we demonstrate that the 2′-OH at A207, a highly conserved nucleotide in the ribozyme active site, specifically stabilizes the chemical transition state by ~2 kcal mol^{-1}. The A207 2′-OH only makes its contribution when the U(−1) 2′-OH immediately adjacent to the scissile phosphate is present, suggesting that the 2′-OHs of A207 and U(−1) interact during the chemical step.

Conclusions: These data support a model in which the 3′-oxyanion leaving group of the transesterification reaction is stabilized by a hydrogen-bonding triad consisting of the 2′-OH groups of U(−1) and A207 and the exocyclic amine of G22. Because all three nucleotides occur within highly conserved non-canonical base pairings, this stabilization mechanism is likely to occur throughout group I introns. Although this mechanism utilizes functional groups distinctive of RNA enzymes, it is analogous to the transition states of some protein enzymes that perform similar phosphoryl-transfer reactions.

Address: Department of Molecular Biophysics and Biochemistry, Yale University, 260 Whitney Avenue, New Haven, CT 06520-8114, USA.

Correspondence: Scott A Strobel
E-mail: strobel@csb.yale.edu

Key words: interference suppression, nucleotide analog interference mapping, phosphoryl transfer, reaction mechanism, self-splicing intron

Received: **1 December 1998**
Revisions requested: **30 December 1998**
Revisions received: **7 January 1999**
Accepted: **13 January 1999**

Published: **17 February 1999**

Chemistry & Biology March 1999, 6:153–165
http://biomednet.com/elecref/1074552100600153

 ISSN 1074-5521

Introduction

Understanding the chemical mechanism of catalysis by RNA enzymes is a subject of particular interest because the nucleotide building blocks that comprise ribozymes are fundamentally different from those of protein enzymes, yet both macromolecules efficiently catalyze phosphoryl-transfer reactions [1]. This raises an intriguing question: do these two very different classes of macromolecular biocatalysts utilize similar strategies to catalyze phosphate transesterification? Although the reaction mechanisms of several protein enzymes that promote phosphoryl-transfer reactions have been elucidated [2], the chemical basis of ribozyme catalysis must be further characterized before a comparison of transition-state mechanisms of protein and RNA enzymes can be completed.

The *Tetrahymena* group I intron catalyzes two phosphate-transesterification reactions in the course of self-splicing (Figures 1,2) [3]. It promotes these reactions with a rate enhancement ~10^{11}-fold over the uncatalyzed rate and with much greater specificity [4]. Both the first and second steps of splicing involve nucleophilic attack by a 3′-OH on a phosphodiester linkage, which displaces a 3′-oxyanion leaving group from the scissile phosphate, and both reactions are catalyzed within the same active site [5].

Alternative constructs of the group I intron have been developed to independently explore both steps of splicing (Figure 2) [6,7]. The L-21 ScaI form of the intron lacks the 5′ and 3′ exons as well as the terminal guanosine, and it has been used to study the first step of splicing (Figure 2a) [6,8]. This enzyme binds exogenous guanosine and an oligonucleotide substrate analogous to the 5′–3′ ligated exons. The second step of splicing has been investigated using the L-21 G414 form of the intron (Figure 2b) [7,9]. It retains the terminal guanosine (G414), which can attack the oligonucleotide substrate and transfer the 3′ exon onto the end of the intron in a reaction analogous to the reverse of the second step of splicing. For both forms of the intron, the binding of the oligonucleotide substrate occurs in two distinct steps [10,11]. First, the oligonucleotide substrate base pairs with the internal guide sequence (IGS) to form the P1 or substrate helix in an open complex (Figures 1,2). This helix docks into the ribozyme active site to form the closed complex where the substrate is cleaved by guanosine.

Experiments to elucidate the chemical basis of group I intron catalysis have focused primarily upon metal ions and the role of particular functional groups located within the two substrates of the ribozyme reaction, that is, the

Figure 1

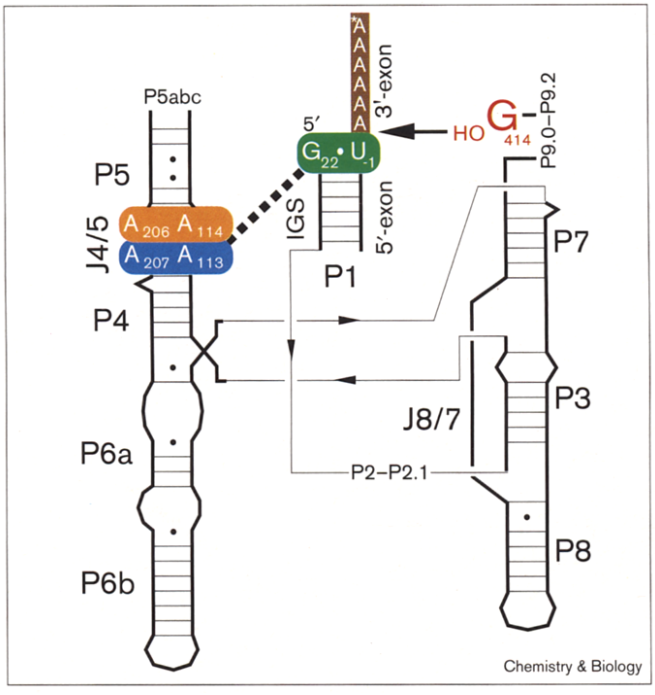

The secondary structure of the *Tetrahymena* group I ribozyme with the G·U wobble pair in P1 (green), the sheared A·A pairs in J4/5 (orange and blue), and the terminal guanosine (red) highlighted.

guanosine cofactor and the P1 duplex comprised of the 5′-exon and the IGS [12–21]. The experiments demonstrate that the group I intron is a metalloenzyme because it requires at least three magnesium ions to stabilize the chemical steps of splicing ([22–26]; S. Shan, A. Yoshida, J.A. Piccirilli and D. Herschlag, personal communication). One metal ion activates the 3′-OH of G for nucleophilic attack [25]. A second interacts with the 2′-OH of G, which might improve the nucleophilicity of the 3′-OH ([26]; S. Shan, A. Yoshida, J.A. Piccirilli and D. Herschlag, personal communication). A third metal ion stabilizes the 3′-OH leaving group of U(–1), which is the terminal nucleotide of the 5′-exon. The two metal ions that coordinate the nucleophile and the leaving group provide a large fraction of the energy required for catalysis, as each enhances the reaction rate by as much as 10,000-fold [24,25].

In addition to the metal ions, specific functional groups within the substrate helix contribute to transition-state stabilization. Six 2′-OH groups in the P1 helix make ground-state tertiary interactions that provide intrinsic binding energy for the transition state [21,27–31]. In addition to these interactions, two functional groups within the highly conserved G22·U(–1) wobble pair adjacent to the 5′-splice site selectively stabilize the chemical step of group I intron splicing. These groups are the 2′-OH of U(–1) and the N2 exocyclic amine of G22 [16,20]. The U(–1) 2′-OH is immediately adjacent to the 3′-oxyanion leaving group of the same nucleotide and accelerates the reaction by more than 1000-fold (~5 kcal mol^{-1}) (Figure 3). Functional group substitution experiments suggested that this hydroxyl group makes its contribution by donating a hydrogen bond to the 3′-oxyanion and that this hydrogen bond only forms during

Figure 2

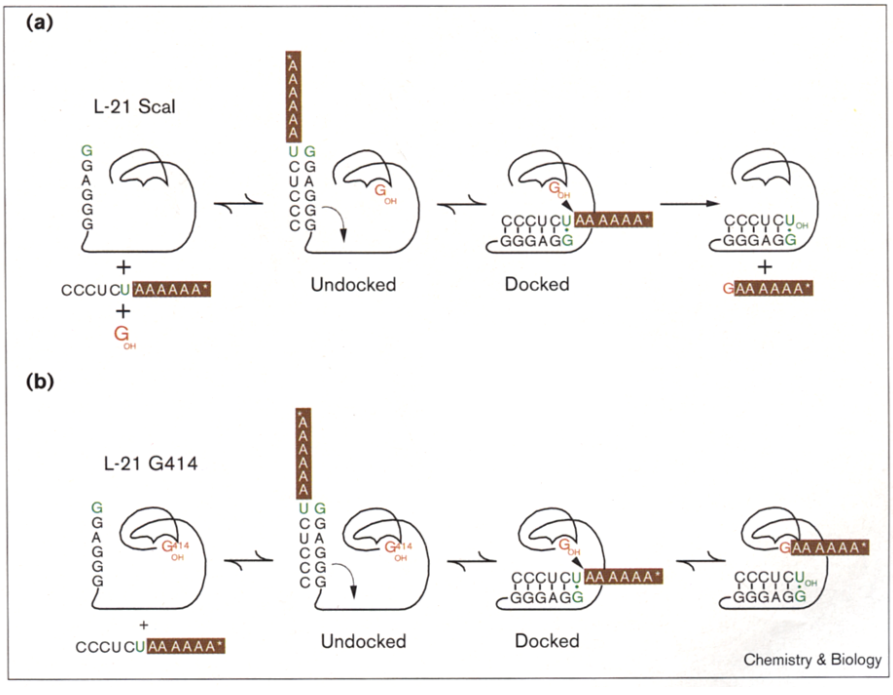

(a) A reaction scheme for the L-21 ScaI reaction, which is analogous to the first step of intron splicing and uses exogenous guanosine as the nucleophile. **(b)** A reaction scheme for the 3′-exon ligation reaction performed by the L-21 G414 form of the group I intron. The reaction is analogous to the reverse of the second step of intron splicing and uses the terminal nucleotide of the intron, G414, as the nucleophile.

Figure 3

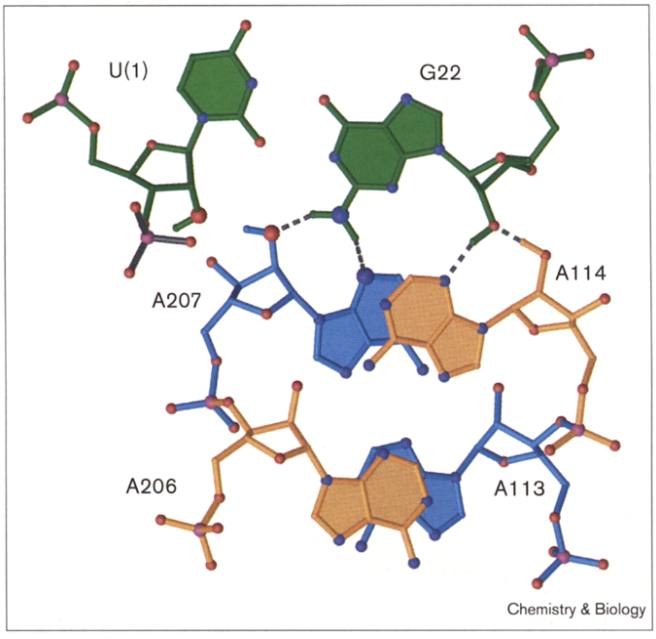

A model of the tertiary hydrogen-bonding interactions between the G·U pair of P1 (green) and the two consecutively stacked sheared A·A pairs of the J4/5 region (orange and blue).

the transition state [16]. Substitution of this 2′-OH has no effect on the binding of the substrate into the active site [16,27,28]. The second important functional group is the G22 exocyclic amine, which acts as a primary determinant of 5′-splice site selection and is the only sequence-specific contact between P1 and the catalytic core [19,20]. The G22 amine makes a substantial contribution to ground-state helix docking (~2.0 kcal mol^{-1}), but it also makes a contribution to the chemical transition state (~1 kcal mol^{-1}).

Experiments involving site-specific substitution of these two important functional groups indicated that there is a small amount of transition-state energy (<0.5 kcal mol^{-1}) attributable to an interaction between them [18,20]. Within a wobble pair, however, these groups are not sufficiently close to form a direct hydrogen-bonding interaction that could account for this energy. A crystal structure of a model duplex containing a G·U pair demonstrated that an ordered water molecule can bridge between the U 2′-OH and G N2 amino groups [32]. This led to the proposal that a water molecule or 2′-hydroxyl group could participate in the chemistry of the group I intron by bridging between the catalytically important groups of the wobble pair [18,32], but the existence of this putative mediating functional group had not been proven.

We recently reported a model for the ground-state docking interactions between the J4/5 region of the ribozyme active site and the G22·U(–1) pair (Figure 1) [33]. In this model the G·U pair utilizes its 2′-OH and N2 amine to make four hydrogen bonds with the convex minor groove surface created by two consecutively stacked sheared A·A pairs in the highly conserved J4/5 internal loop (Figure 3). This interaction places the 2′-OH of nucleotide A207 between the two functional groups known to contribute to chemistry. It occupies approximately the same position as the water molecule observed within the crystal structure of a G·U wobble pair [32]. Based upon its location within the G·U wobble pair, it seems plausible that the 2′-OH of A207 also contributes to the chemical step of splicing. In this report, we demonstrate that there is a hydrogen-bonding triad between the exocyclic amine of G22 and the 2′-OHs of U(–1) and A207, and that this network of interactions selectively stabilizes the chemical transition state of the *Tetrahymena* group I intron.

Results

Nucleotide analog interference mapping

The P1-J4/5 ground state docking model led to the hypothesis that the 2′-OH of A207 might participate directly in the chemistry of group I intron splicing (Figure 3) [33]. Our initial experiments to demonstrate such a role involved the use of nucleotide analog interference mapping (NAIM), a chemogenetic method that makes it possible to rapidly identify the chemical groups responsible for RNA function (Figure 4) [34,35]. NAIM involves random low level incorporation of an α-phosphorothioate-tagged nucleotide analog into the intron by T7 RNA polymerase and selection of the resulting transcripts for splicing activity. The active introns are treated with iodine to cleave the phosphorothioate linkage and the fragments are analyzed using polyacrylamide gel electrophoresis (PAGE) [36]. If incorporation of a nucleotide analog at a particular site impairs activity, it can be rapidly identified by disappearance of a specific band within the RNA sequencing ladder (Figure 4). The L-21 G414 form of the *Tetrahymena* group I intron is particularly amenable to this experimental approach because it can transfer the 3′-end of a radiolabeled oligonucleotide substrate onto its 3′ end, thus marking the active introns in the population with a radioactive tag (Figure 2b) [35].

Previous experiments using dAαS [5′-*O*-(1-thio)-2′-deoxyadenosine monophosphate] and ^{F}AαS [5′-*O*-(1-thio)-2′-deoxy-2′-fluoroadenosine monophosphate], in which the 2′-OH of A is replaced with a proton and with a fluorine, respectively, revealed an interference pattern at A207 that was essential for modeling the P1-J4/5 interaction [33]. Strong interference was observed with dAαS at A207, but ^{F}AαS incorporation at A207 resulted in slight enhancement of activity. Because the highly electronegative 2′-fluoro group can still accept a hydrogen bond, such an interference pattern argued that the 2′-OH of A207 is a hydrogen-bond acceptor. Interference-suppression experiments supported this prediction by demonstrating that the

Figure 4

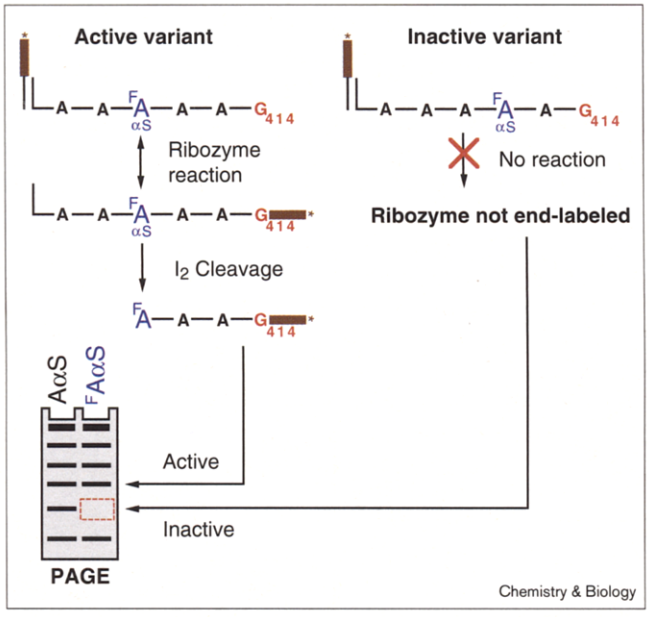

Nucleotide analog interference mapping (NAIM) using the 3′-exon ligation reaction as the selection step.

Figure 5

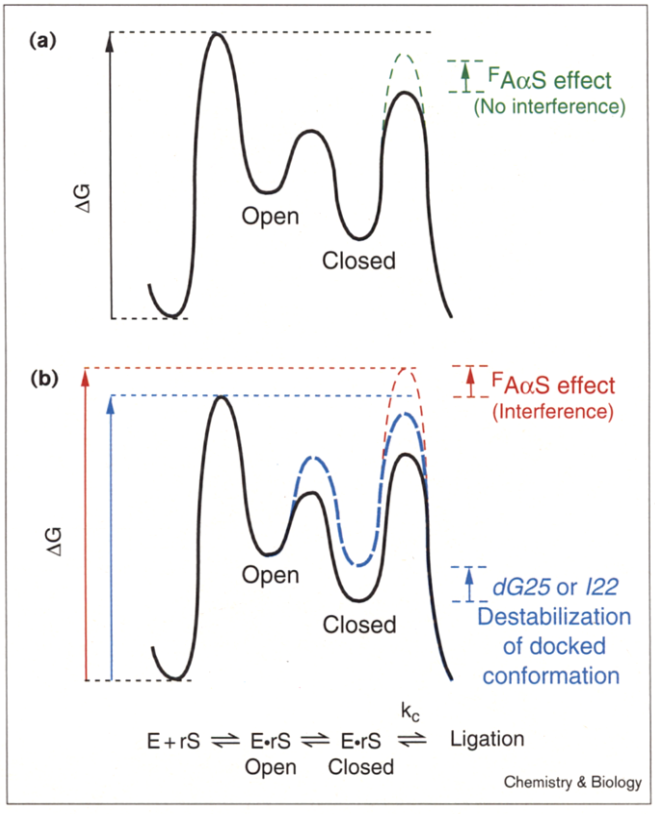

Free-energy profiles for substrate binding, docking and chemical transformation for **(a)** the wild-type and **(b)** the *dG25*- and *I22*-substituted ribozymes.

A207 2′-OH accepts a hydrogen bond from the G22 amino group (inosine substitution at position 22 partially suppressed dAαS interference at A207) [33]. There was still no direct data to demonstrate that the 2′-OH groups of A207 and U(–1) interact, although their proximity in the model (~3.0–3.5 Å) implied that such an interaction was structurally reasonable with a modest realignment of the nucleotides (Figure 3).

Interference mapping at A207 when the chemical step is limiting

If A207 bridges between U(–1) and G22 in the chemical step, we expected that it would act as a hydrogen-bond donor to the U(–1) 2′-OH. ^{F}AαS should therefore show interference under conditions when chemistry is the limiting step in the reaction. This was not observed in the results reported previously; but those experiments were performed using a substrate with a 2′-deoxy substitution at the cleavage site. Although chemistry is limiting under those conditions, the substrate lacks the U(–1) 2′-OH that is expected to participate in the critical interaction. We repeated the experiments using a substrate containing the U(–1) 2′-OH, but again failed to detect ^{F}AαS interference at A207 despite testing several reaction conditions, including low pH and low Mg^{2+} concentrations (data not shown). This can be explained by the fact that for cleavage of an all ribose substrate by a population of ribozyme variants that are each present at very low concentration, substrate binding rather than chemistry is the limiting step of the reaction [8,37]. Functional groups that moderately disrupt chemistry would not be expected to show interference under such conditions (Figure 5a, green).

The kinetic profile of the reaction predicts that ^{F}AαS will only cause interference at A207 if the experiments are performed using a substrate with a ribose at the cleavage site under conditions in which chemistry is limiting. To achieve this condition, we prepared ribozymes that were impaired in their ability to dock the P1 helix into the ribozyme active site [19,30]. Because destabilization of the docked ground-state complex equally disrupts the chemical transition state, the energetic barrier for chemistry is raised to the point that it approaches the energetic barrier for substrate binding (Figure 5b, blue). Upon reaching the docked complex, these impaired ribozymes are more likely to dissociate than the wild-type enzyme. Dissociation is even more favored if the energy of the chemical transition is further increased by loss of a particular functional group that contributes to the chemical step (Figure 5b, red).

To determine the role of the A207 2′-OH using NAIM we prepared two sets of ribozymes impaired in their ability to dock the P1 helix. Each set of ribozymes lacks a specific

functional group important for P1 helix docking into a different region of the active site [30,38]. One set of ribozymes contained an inosine at position 22 (I22), which lacks the exocyclic amine important for P1 docking into J4/5 [19,33]. The second set of ribozymes contained a 2′-deoxy substitution at G25, which lacks a 2′-OH important for P1 helix docking into the single-stranded segment J8/7 [30,39]. Both RNAs were transcribed with either AαS or ^{F}AαS randomly incorporated throughout the length of the transcript to test for interference at A207 and other positions in the RNA. A total of four enzymes were prepared: *I22 AαS*, *I22 ^{F}AαS*, *dG25 AαS* and *dG25 ^{F}AαS*.

The substituted L-21 G414 ribozymes were assayed for interference using a 3′-end-labeled substrate with a ribose at the cleavage site (r1d45S; CdCdCUCrTAAAAA). The 2′-deoxynucleotide substitutions at –4 and –5 were included to eliminate miscleavage of the substrate due to the I22 and dG25 substitutions [11,20,40]. Following the 3′-exon ligation reaction, the RNAs were treated with iodine, and the cleavage products resolved using PAGE to determine the effect of ^{F}AαS substitution at A207 and other positions within the ribozyme.

In contrast to the previous experiments, where either chemistry was not rate-limiting or the substrate lacked a 2′-OH at the cleavage site, both the *I22* and *dG25* ribozymes displayed significant ^{F}AαS interference at A207 (Figure 6a). Neither of these enzymes showed AαS interference at this position, indicating that the effect is specifically due to the 2′-fluoro substitution and not a phosphorothioate effect. Furthermore, no other changes in the interference pattern were detected in comparison with the results published previously, which used a substrate with a 2′-deoxy nucleotide at the cleavage site [33,41]. The fact that ^{F}AαS interference is seen with both the *I22* and *dG25* ribozymes argues that it is not dependent upon the specific modification introduced to destabilize the docked ground state of the reaction. These data support a mechanism in which a hydrogen-bond donor at the 2′-OH position of A207 is important for ribozyme function, but only under conditions in which chemistry is the rate-limiting step.

A207 interference suppression by 2′-deoxy substitution at U(–1)

To determine how the A207 2′-OH participates in the chemical step, we performed an interference suppression experiment. NAIS is an extension of NAIM that employs the logic of genetics to identify specific hydrogen-bonding partners within an RNA tertiary structure [33]. In principle, if an interaction is disrupted by deletion or alteration of one functional group in an interacting pair, then no significant energetic penalty will result from deletion or alteration of the second functional group. The suppression of an interference effect can be detected by the reappearance of a specific band on the sequencing gel (Figure 4).

The transition-state model predicts that the 2′-OH of A207 donates a hydrogen bond to the 2′-OH of U(–1). On the basis of this model, deletion of the hydroxyl group at the cleavage site should eliminate any positive contribution made by the hydroxyl group at A207. This would be observed experimentally as A207 ^{F}AαS interference suppression resulting from elimination of the U(-1) 2′-OH. To test this possibility, the *I22* and *dG25* ribozymes were again assayed for interference using a substrate with a 2′-deoxy substitution at the cleavage site (d145S; CdCdCUCdTAAAAA). In contrast to the results described above, the substrate with a 2′-deoxynucleotide did not show interference at A207 with ^{F}AαS (Figure 6). This is true in spite of the fact that d145S is more than 1000-fold less reactive than r1S, and thus the reaction conditions were significantly more selective than those used for the all-ribose substrate. Furthermore, the site of interference suppression was specific, in that ^{F}AαS interference at A218 (Figure 6) and other control sites within the intron were not suppressed by the 2′-deoxy substitution at the cleavage site (data not shown). ^{F}AαS interference suppression at A207 was observed for both the *I22* and the *dG25* ribozymes, which confirms that the effect is independent of the type of substitution used to destabilize the docked ground-state conformation. These data argue that the 2′-OH groups at A207 and U(–1) interact during the chemical transition state, most likely via a direct hydrogen bond.

Characterization of A207-substituted ribozymes

Interference and suppression data provide only qualitative evidence that the 2′-OH of A207 participates in the chemistry of group I intron splicing. To measure the A207 2′-OH contribution directly, we prepared L-21 ScaI ribozymes with a specific 2′-deoxy or 2′-fluoro substitution at A207 and measured kinetic and thermodynamic constants for the site-specifically substituted ribozymes. The L-21 ScaI form of the ribozyme binds an oligonucleotide substrate and uses exogenous guanosine to cleave at the 5′-splice site (Figure 2a) [6,8]. This reaction is analogous to the first, rather than the second, step of splicing, so these experiments make it possible to determine if the A207 2′-OH is also important for the first step of intron splicing. The A207-substituted ribozymes were prepared semisynthetically by a three-piece ligation of two truncated RNA transcripts and a 9-mer synthetic oligoribonucleotide containing either adenosine (rA), 2′-deoxyadenosine (dA) or 2′-deoxy-2′-fluoroadenosine (^{F}A) at A207 to produce ribozymes *rA207*, *dA207* and *^{F}A207*, respectively. The overall yield of the ligation reaction was only about 2% despite extensive efforts to optimize the ligation conditions (see the Materials and methods section).

The P1 helix docking model predicts that the A207 2′-OH accepts a hydrogen bond from the N2 amine of G22 in the ground state [33] (Figure 3). This should be manifest as a reduction in oligonucleotide substrate affinity by the *dA207*

Figure 6

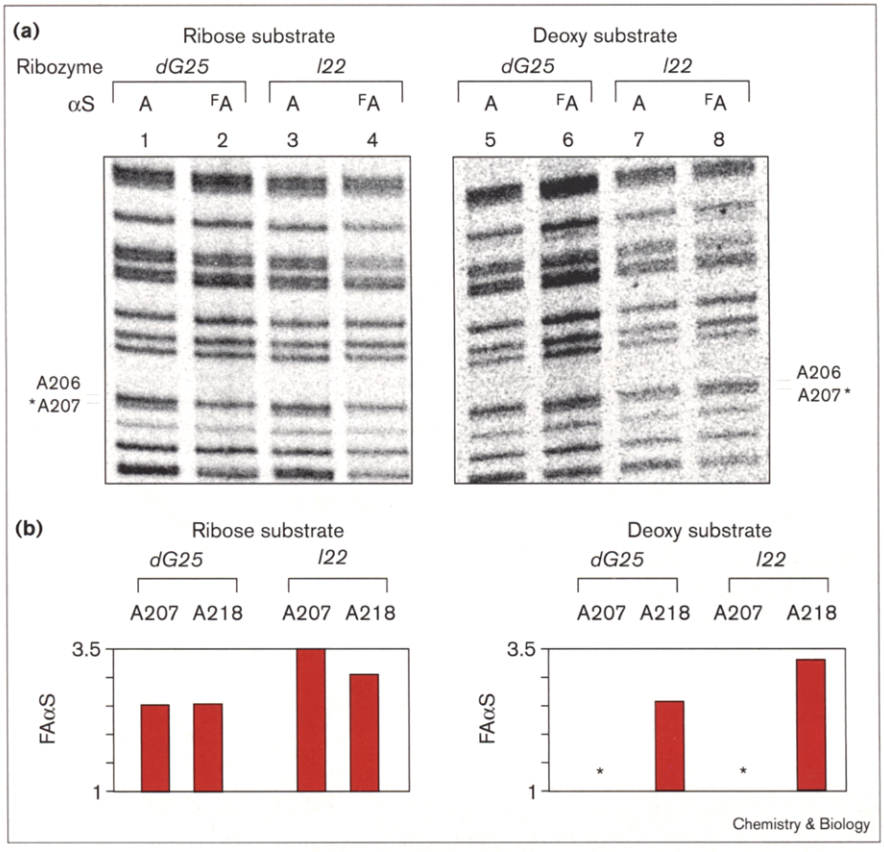

(a) NAIM for the *dG25*- and *I22*-substituted ribozymes with the analogs AαS and ^{F}AαS using the substrates r1d45S (ribose substrate) or d145S (deoxy substrate). The cleavage band for A207 is marked with an asterisk. Note that the band is missing in the ^{F}AαS lanes with the ribose substrate (lanes 2 and 4), but is present in the ^{F}AαS lanes with the deoxy substrate (lanes 6 and 8). **(b)** Histogram depicting the magnitude of ^{F}AαS interference at A207 and A218 for the *dG25*- and *I22*-substituted ribozymes.

ribozyme, whereas ^{F}*A207* would not show the effect because it still has a hydrogen-bond acceptor available for the G22 amino group. To test this prediction, we measured the equilibrium dissociation constants of the *rA207*, *dA207* and ^{F}*A207* ribozymes for the oligonucleotides r1P (GGCCCUCrT) and d1P (CCCUCdT; Table 1) [42]. *rA207* bound both oligonucleotides with the same affinity as the fully transcribed L-21 ScaI RNA, which demonstrates that there are no unexpected effects resulting from ribozyme preparation by three-piece ligation. Consistent with the P1 docking model (Figure 3), *dA207* showed a modest 0.4–0.8 kcal mol^{-1} loss of binding energy for both substrates, whereas ^{F}*A207* was at least as stable as the all-ribose enzyme. The magnitude of the *dA207* effect is consistent with that expected for deletion of this functional group, because the G22 amine contributes 2 kcal mol^{-1} and it interacts with both the 2′-OH and N3 of A207, whereas the 2′-deoxy substitution at A207 only eliminates one of these interactions [19,33]. The observation that the dA207 substitution is less destabilizing with a ribonucleotide than with a deoxynucleotide at the cleavage site (0.4 compared with 0.8 kcal mol^{-1}, respectively, Table 1) is further evidence against a ground-state hydrogen bond between the A207 and U-1 2′-OH groups. The lack of an effect from 2′-fluoro substitution quantitatively confirms that the 2′-OH of A207 acts as a hydrogen-bond acceptor in the ground state as predicted in the P1 docking model (Figure 3) [33].

We further characterized the A207-substituted ribozymes kinetically to determine if there is any effect on the chemical step. We initially measured the second-order rate constant $(k_{cat}/K_m)^G$ for cleavage of the all-ribose substrate r1S (GGCCCUCrTAAAAA), which under single-turnover conditions represents the rate of reaction for E^S (substrate fully bound to the ribozyme, but the G-binding site unoccupied) with free G. For the wild-type ribozyme under these conditions, $(k_{cat}/K_m)^G$ is limited by a combination of

Table 1

Equilibrium dissociation constants for oligonucleotide binding by the A207-substituted L-21 ScaI ribozymes.

Ribozyme	K_d (nM) r1P	ΔΔG kcal mol^{-1}	K_d(nM) d1P	ΔΔG kcal mol^{-1}
Wild-type	7.1 ± 1.1	–	10.9 ± 0.9	–
rA207	8.8 ± 2.3	0.1	13.2 ± 1.1	0.1
dA207	14.6 ± 1.0	0.4	42.2 ± 3.1	0.8
^{F}*A207*	6.8 ± 4.0	0.0	10.5 ± 5.1	0.0

Table 2

Kinetic characterization of the A207-substituted ribozymes.

Ribozyme	$(k_{cat}/K_m)^G$ ($10^4 M^{-1}min^{-1}$)	K_{rel}	K_mG (μM)	$k_{chem}(min^{-1})$ r1S	ΔΔG kcal mol^{-1}	$k_{chem}(min^{-1})$ d1S	ΔΔG kcal mol^{-1}
Wild-type	14 ± 2	–	90	15	–	0.0044 ± 0.0002	–
rA207	13 ± 3	1.1				0.0043 ± 0.0002	0.0
dA207	0.42 ± 0.05	3.3	170 ± 30	0.68 ± 0.04	1.9	0.0028 ± 0.0002	0.3
^{F}A207	0.20 ± 0.02	7.0	130 ± 10	0.44 ± 0.02	2.1	0.0038 ± 0.0003	0.1

guanosine binding and chemistry [8,43]. Although *rA207* reacted at a rate equivalent to that of the wild-type RNA, both the *dA207* and *^{F}A207* ribozymes were more than 30-fold less efficient at substrate cleavage (Table 2).

Because this observed decrease in the cleavage rate might be caused by a reduction in G affinity (K_m^G effect) or a reduction in the rate of chemistry (k_{cat} effect), we measured k_{obs} at several guanosine concentrations and calculated k_{cat} and K_m for the reaction (Figure 7, Table 2). Under these conditions K_m is equal to the K_d for guanosine binding and the k_{cat} is equal to k_{chem}, the rate of the chemical step [20,43,44]. The kinetic data indicate that K_m^G for the *dA207* and *^{F}A207* ribozymes is less than twofold higher than the wild-type ribozyme, which argues against a direct participation of the A207 2′-OH in G binding (Table 2). In contrast, k_{cat} of r1S cleavage was 22- and 34-fold lower for *dA207* and *^{F}A207*, respectively. This represents at least a 2 kcal mol^{-1} loss in transition-state stabilization energy specific to the chemical step. Because the effect is observed with both the 2′-fluoro and 2′-deoxy substitutions, it argues that the 2′-OH of A207 donates a hydrogen bond in the chemical step.

Figure 7

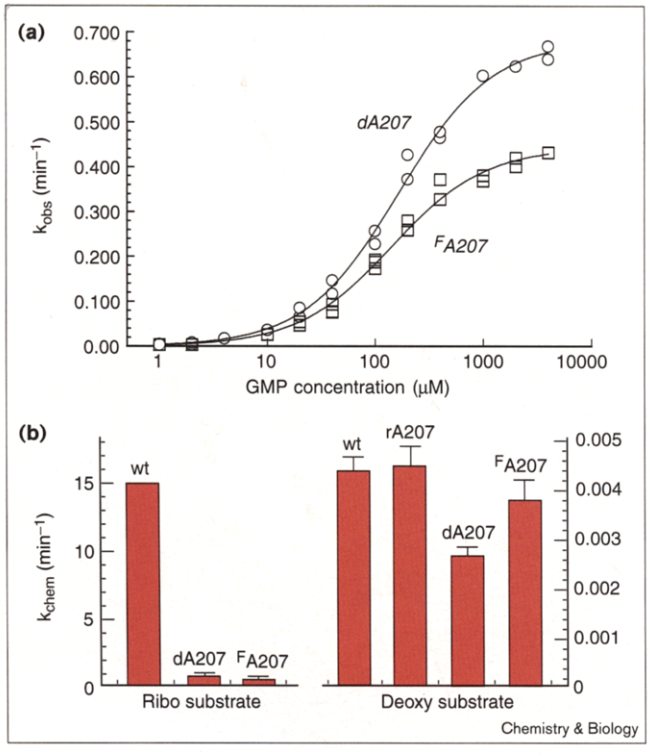

(a) A plot of k_{obs} versus [GMP] for the cleavage of r1S by the *dA207*- and *^{F}A207*-substituted ribozymes. **(b)** A histogram of k_{cat} values for the cleavage of oligonucleotide substrates r1S (ribo substrate) and d1S (deoxy substrate) by wild-type (wt) and A207-substituted ribozymes. Note that the scale on the y axis differs for the two substrates.

The interference-suppression experiments suggested that the A207 2′-OH interacts with the 2′-OH of U(–1) during the chemical step. To determine if the A207 substitutions still have an effect on chemistry when there is a 2′-deoxy group at the cleavage site, we measured k_{cat} for the substrate d1S at saturating enzyme and saturating guanosine concentrations (Figure 7, Table 2). Under these conditions, k_{cat} is again equal to the rate of chemistry (k_{chem}). As expected, all the ribozymes cleaved the single 2′-deoxy-substituted substrate more than 1000-fold slower than they cleaved the all-ribose substrate; but there was no additional loss of chemical transition-state energy resulting from modification of the 2′-OH at A207 (k_{chem} for *dA207* and *^{F}A207* was not even twofold less than that of the wild-type ribozyme). Together these data suggest that the 2′-OH of A207 contributes about 2 kcal mol^{-1} to chemistry by donating a hydrogen bond to the 2′-OH of U(–1).

Discussion

Model of the group I ribozyme chemical transition state

Previous models of the group I intron chemical transition state have proposed that the 2′-OH adjacent to the scissile phosphate interacts with a metal ion, a water molecule or a specific functional group within the catalytic core of the ribozyme during the chemical step [18,32]. The interference and single-site substitution experiments described here support a model in which the 2′-OH of U(–1) accepts a hydrogen bond from the 2′-OH of A207, a functional group located within the ribozyme active site. The A207 2′-OH represents the first functional group within the catalytic core of the group I that has been shown to participate directly in the stabilization of the chemical transition

Figure 8

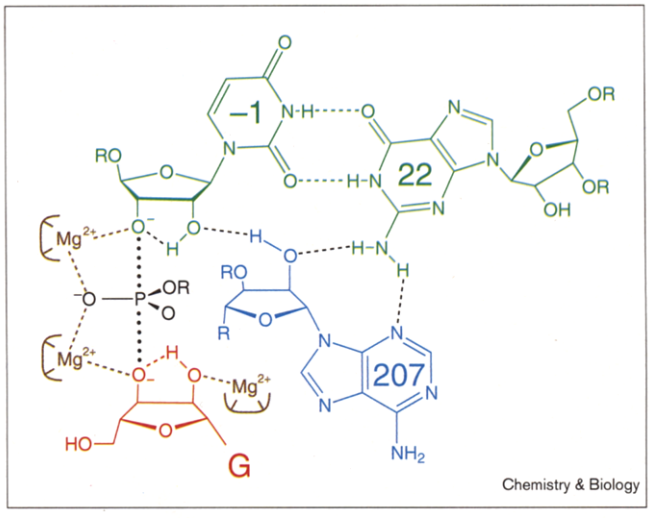

Model of the *Tetrahymena* group I intron chemical transition state involving a hydrogen-bonding triad between the 2′-OH groups of U(−1) and A207, and the exocyclic amine of G22.

state. In addition to forming a transition-state hydrogen bond with U(−1), the A207 2′-OH also makes a ground-state hydrogen bond that is most likely retained in the chemical step with the G22 N2 amino group. This series of interactions therefore defines a hydrogen-bonding triad between the functional groups of three nucleotides: U(−1), A207 and G22. All three of the nucleotides in the network are at least 99% conserved among group I introns [45]. Each nucleotide is located within a noncanonical base pair that is also highly conserved, including the G22·U(−1) wobble pair at the cleavage site and the A207·A113 sheared pair in the active site. This suggests that the hydrogen-bonding triad is likely to be a conserved catalytic component of almost all group I introns.

Although these biochemical experiments cannot completely rule out the possibility that a water molecule or metal ion might mediate the interaction between these groups, all of the tertiary contacts between P1 and the J4/5 region can be accommodated with reasonable distances and geometries by invoking direct hydrogen bonds between the functional groups (Figure 3). The G·U docking model into J4/5 is based upon an intermolecular interaction within the P4–P6 crystal structure, and the distances and geometries within that structure are inconsistent with water- or metal-mediated interactions [33,46]. Furthermore, the biochemical experiments define which functional groups act as hydrogen-bond donors or acceptors, and this relationship can be properly maintained within the triad model without invoking a metal ion. The simplest model based upon the biochemical and structural data is therefore that the functional groups in the triad make direct hydrogen-bonding interactions.

A model for the *Tetrahymena* group I ribozyme transition state that incorporates these data with previous studies is shown in Figure 8 [47]. In addition to stabilization by a metal ion, the 3′-oxyanion is activated by the hydrogen-bonding triad. Previous studies on the pH profile of the reaction suggested that the U(−1) 2′-OH does not donate a proton to the leaving group (general acid mechanism), but rather that it stabilizes the developing negative charge by a hydrogen-bonding mechanism [16]. This network of interactions involving the 2′-OH of A207 might increase the ability of the U(−1) 2′-OH to serve as a hydrogen-bond donor by lowering the pK_a of the hydroxyl group, or it might make an entropic contribution by restricting the rotational freedom of the U(−1) 2′-OH for hydrogen bonding to the 3′-oxyanion [18,32]. Because RNA lacks functional groups with pK_a values near neutrality, a hydrogen-bonding network might provide a viable alternative to a general acid mechanism by dissipating a negative charge across several functional groups.

An alternative set of interactions appears to activate the 3′-nucleophile of G (Figure 8; [26,48]; S. Shan, A. Yoshida, J.A. Piccirilli and D. Herschlag, personal communication). In addition to direct metal-ion coordination, the 3′-oxyanion nucleophile is likely to accept a hydrogen bond from the adjoining 2′-OH group of G. This conclusion is based upon the observation that 2′-deoxyguanosine is a competitive inhibitor of the splicing reaction [48]. The 2′-OH of G is, in turn, coordinated to a third metal in the active site [26] (S. Shan, A. Yoshida, J.A. Piccirilli and D. Herschlag, personal communication). This implies that on the G side of the transesterification reaction a metal ion might take the place of the hydrogen-bonding network.

The interference and single-site substitution data indicate that the same hydrogen-bonding network stabilizes both the first and second steps of splicing, consistent with the observation that both reactions are catalyzed within the same active site [5]. The forward and the reverse of the second step of splicing are energetically equivalent with an equilibrium constant of ~1 [9]. This implies that the hydrogen-bonding triad also stabilizes the deprotonated form of the 3′-oxyanion nucleophile during the exon-ligation step of splicing. The triad is therefore predicted to be responsible for stabilizing the leaving group during the first step of splicing and for activating the nucleophile during the second step of splicing.

Based upon the ground state docking model for the P1 interaction with the J4/5 region, it is intriguing to speculate on the magnitude of the conformational change required for the ribozyme to form the catalytic tertiary interaction in the chemical transition state. Because ground-state docking interactions were predictive of a transition-state tertiary contact, it argues against a large conformational change within the J4/5 region of the active site [33].

Instead, small changes in the conformation of the A207 or U(–1) ribose sugars might alone be sufficient to align these groups for chemistry. Although it remains possible that larger conformational rearrangements are required outside of the J4/5 region in order to bring the catalytic metals into proper alignment for chemistry, the P1-J4/5 interaction appears to be largely pre-ordered within the docked ground-state complex.

Energetic contribution of individual groups in the hydrogen-bonding triad

This hydrogen-bonding network stabilizes the chemical transition state by almost 6 kcal mol^{-1}. It can be divided into the contributions made by each of the functional groups based upon these and results published previously [15,16,18–20]. The most significant functional group is the 2′-OH of U(–1). Deletion of this group reduces the rate of the chemical reaction by almost 5 kcal mol^{-1} [15,16]. A substantial fraction of this energy is derived from the hydrogen-bonding network, because the net contribution is reduced to 3 kcal mol^{-1} if the 2′-OH of A207 is deleted (2.9 kcal mol^{-1} for *^{F}A207* and 3.3 kcal mol^{-1} for *dA207*). At the other end of the hydrogen-bonding triad, the G22 amine contributes slightly more than 1 kcal mol^{-1} to chemistry [19,20]. It interacts with the N3 and 2′-OH groups of A207 in the ground state, and these hydrogen bonds appear to be strengthened by about 0.7 kcal mol^{-1} in the chemical step [20,33]. This fraction of the energy is independent of a intact triad because it is not affected by deletion of the U(–1) 2′-OH. The remainder of the energy (0.4 kcal mol^{-1}) is lost, however, when the U(–1) 2′-OH is removed [18,20]. The ribozyme therefore provides slightly less than 3 kcal mol^{-1} (2 kcal mol^{-1} from A207 2′-OH and 0.7 kcal mol^{-1} from G22 amine) of activation energy through this ensemble of hydrogen bonds. The remainder of the energy (about 3 kcal mol^{-1}) is provided by the U(–1) 2′-OH, although this functional group is part of the substrate, so in a formal sense it does not contribute to the catalytic potential of the intron.

According to transition-state theory, catalysis requires stabilization of a reaction's transition state without equivalent stabilization of the reaction's ground state [49,50]. This criterion is met by the hydrogen-bonding triad because the U(–1) 2′-OH does not make an energetically significant interaction with the A207 2′-OH in the ground state. There is no effect on ground-state binding upon U(–1) 2′-deoxy substitution in the substrate [27–29] or A207 2′-fluoro substitution in the ribozyme despite the fact that either one of these substitutions would destabilize any potential interaction between these groups. By contrast, the equivalent substitutions have a significant effect on the chemical step. This interaction is therefore categorically different from the ground-state hydrogen bonds between P1 and the catalytic core that provide intrinsic binding energy for the transition state [51,52].

Comparison to protein-catalyzed phosphoryl-transfer reactions

It is interesting to compare the chemical basis of RNA catalysis in the group I intron with the mechanism of analogous reactions performed by protein enzymes [1,2]. Obviously, proteins create catalytic centers from an entirely different collection of functional groups than those available to RNA. Although no protein enzymes are known to catalyze exactly the same reactions as those of the group I intron, they do catalyze several phosphoryl-transfer reactions that are similar.

The role of metal ions in RNA and protein active sites has been reviewed elsewhere [2,53]. What is of primary interest to the present work, however, is the role that hydrogen-bonding networks play in catalyzing phosphoryl-transfer reactions within protein active sites. The transition states of two proteins, the 3′–5′ exonuclease subunit from *Escherichia coli* DNA polymerase and fructose-1,6-biphosphatase (FBP), both utilize a network of hydrogen-bonding groups to catalyze their phosphoryl-transfer reactions. The transition-state models for both enzymes are shown in Figure 9 where they have been oriented to facilitate comparison with the ribozyme reaction (Figure 8). Although none of these hydrogen-bonding networks are exactly equivalent, they provide a useful mechanistic comparison between protein- and RNA-mediated catalysis.

The protein-catalyzed reaction that most closely parallels that of group I splicing is the 3′–5′ exonuclease activity of *E. coli* DNA polymerase (Figure 9a) [54,55]. In this example of a phosphoryl-transfer reaction, the 3′-oxyanion is activated by a catalytic metal ion (metal B) and not by protein sidechains. The hydroxide nucleophile, which is activated by coordination to a metal ion (metal A), also forms a network of hydrogen-bonding interactions, however. Glu357 accepts a hydrogen bond from the nucleophilic hydroxide ion and donates a hydrogen bond to the 3′-OH of the terminal nucleotide, creating an abbreviated version of a hydrogen-bonding network seen in the ribozyme. In this comparison, the 3′-OH of the terminal residue in the 3′–5′-exonuclease transition state is analogous to the A207 2′-OH.

The metabolic enzyme fructose-1,6-biphosphatase (FBP) also catalyzes a phosphoryl-transfer reaction. In this example, a hydrogen-bonding network appears to be solely responsible for stabilization of the oxyanion leaving group [56]. Although two metal ions polarize the non-bridging oxygens of the phosphate, they do not directly coordinate the oxyanion (Figure 9b). Instead, the 1-oxyanion is activated by hydrogen bonding to the neighboring 2-OH of the fructose sugar [57]. The 2-OH in turn accepts a hydrogen bond from the carboxylate group of Asp121 [58]. The hydrogen-bonding network of FBP is in many ways analogous to that of the ribozyme, in that the 2-OH

Figure 9

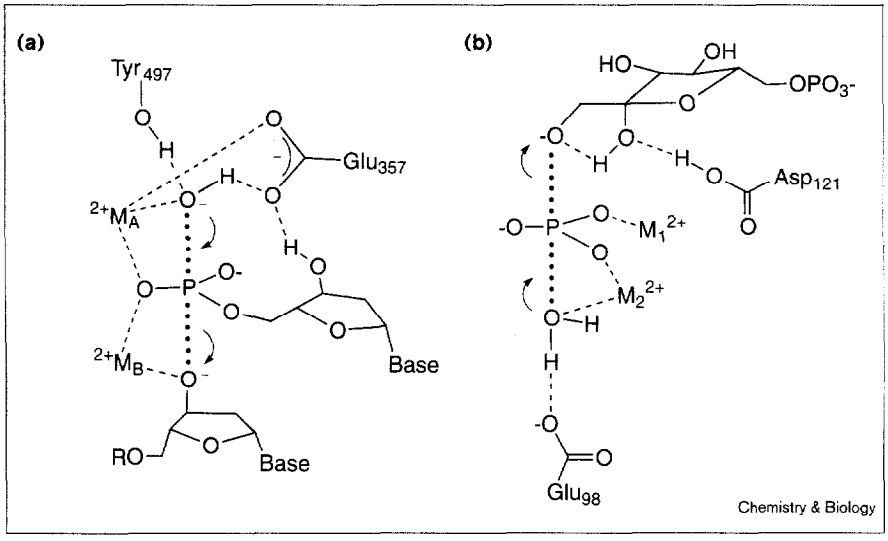

Transition-state models for phosphoryl-transfer reactions catalyzed by **(a)** the 3′–5′ exonuclease domain of *E. coli* DNA polymerase and **(b)** fructose-1,6-biphosphatase.

of the fructose is equivalent to the 2′-OH of U(–1) in the 5′-exon, and Asp121 plays a role similar to that of the A207 2′-OH. A corollary to the G22 exocyclic amine has not been proposed within FBP.

In these two examples of protein-mediated catalysis, the anion leaving group is stabilized by an ensemble of hydrogen bonds rather than by direct protonation by a protein sidechain (general acid mechanism). The observation that an RNA enzyme employs a catalytic strategy analogous to that of proteins reinforces the importance of hydrogen-bonding networks in transition-state stabilization. Such networks might be particularly important for RNA catalysts as they lack titratable functional groups near neutral pH. This result suggests that despite the chemical differences between protein and RNA residues, the functional groups of both macromolecules can be arranged to create mechanistically comparable active sites.

Significance

The mechanism of RNA-mediated catalysis is an issue of significant biochemical interest, particularly in comparison with the catalytic strategies employed by proteins that perform similar phosphoryl-transfer reactions. In this work, we demonstrate that the transition state of the *Tetrahymena* group I ribozyme is, in part, stabilized by an extended network of hydrogen bonds that help stabilize the 3′-oxyanion leaving group. This hydrogen-bonding triad includes two functional groups within the substrate helix (P1), and one within the ribozyme active site that bridges between them. The 2′-OH of A207, which is located in the highly conserved J4/5 segment, is the first group identified in the intron active site that specifically stabilizes the chemical transition state. The hydrogen-bonding network provides almost 3 kcal mol^{-1} of chemical potential to the reaction, and stabilizes both steps of group I intron splicing. Because all three nucleotides [G22, A207 and U(–1)] are highly conserved, and all three are located within conserved noncanonical base pairs, this mechanism for transition-state stabilization is likely to be employed throughout the group I family of self-splicing introns. Based upon comparison with the ground-state model for P1 helix docking, minor structural rearrangements within the J4/5 region appear to be sufficient for the ribozyme to progress from the docked ground state to the chemical transition state of the reaction. The hydrogen-bonding network in the ribozyme transition state has mechanistic parallels to that of the protein enzymes 3′–5′ exonuclease and fructose-1,6-biphosphatase, which employ similar networks to stabilize their chemical transition states. This observation suggests that, despite the chemical differences between protein and RNA residues, the functional groups of both macromolecules can be arranged to create mechanistically comparable active sites.

Materials and methods

Materials

The phosphorothioate-tagged nucleoside triphosphates were purchased from Amersham (ATPαS and dATPαS) or synthesized as previously described previously (^{F}ATPαS) [59]. The oligonucleotide substrates used in the ribozyme reactions and the nine-base oligonucleotides used for preparation of the rA207 and dA207 ribozymes were synthesized by Dharmacon Inc. using 2′-ACE chemistry, and deprotected according to manufacturer's recommendation [60]. No further purification was necessary prior to use. The 17-mer oligonucleotides used to introduce site-specific substitutions in the IGS and the 9-mer oligonucleotide containing the single 2′-deoxy-2′-fluoroadenosine substitution at A207 were prepared by 2′-TBDMS chemistry, deprotected and purified as described

previously. The phosphoramidite of 2′-deoxy-2′-fluoroadenosine necessary to prepare the ^{F}A207 ribozyme was obtained as a generous gift from Isis Pharmaceuticals.

Preparation of I22 and dG25 ribozymes containing AαS and ^{F}AαS

The L-21 G414 ribozymes were prepared semisynthetically by ligating a 17-mer oligonucleotide containing either an I22 or dG25 substitution onto the 5′-end of a truncated L-38 G414 transcript [30]. The L-38 G414 RNA was transcribed *in vitro* from the *EarI* cut plasmid pUCL-38G414 . AαS or ^{F}AαS substitutions (5% incorporation) were introduced randomly into the RNA by adding 5′-O-(1-thio)adenosine triphosphate or 5′-O-(1-thio)-2′-deoxy-2′-fluoroadenosine triphosphate in the transcription reaction as described previously [59]. ^{F}AαS incorporation required the use of the Y639F mutant T7 RNA polymerase, which efficiently incorporates nucleotides modified at the 2′ position [59,61]. GMP (5 mM, 1 mM NTPs) was included in the transcription reaction to create a free 5′-phosphate for ligation onto the 17-mer oligonucleotide. The RNAs were purified by PAGE (6% acrylamide, 7 M urea), eluted from the gel into TE (10 mM Tris–HCl, 0.1 mM EDTA, pH 7.5), desalted and concentrated. The ligation reaction was performed using 1 nmole of L-38 G414 RNA, 2 nmoles of oligoribonucleotide, 2 nmoles of DNA splint oligonucleotide, and T4 DNA ligase (100 units) as previously described for preparation of semisynthetic L-21 ScaI RNAs [30]. The four ligated L-21 G414 RNAs (I22 AαS, I22 ^{F}AαS, dG25 AαS, or dG25 ^{F}AαS) were purified by PAGE (5% acrylamide, 7 M urea), eluted into TE, ethanol precipitated, redissolved in TE and stored at −20°C.

Interference mapping and interference suppression

The oligonucleotide substrates d145S (5′-CdCdCUCdTAAAAA-3) and r1dC45S (5′-CdCdCUCUAAAAA-3′) were radiolabeled at their 3′-ends with yeast poly-A-polymerase and ^{32}P-α-cordycepin [62]. Both oligonucleotides were purified by PAGE (10% acrylamide, nondenaturing) and eluted into TE. For ease of synthesis, d145S has dT instead of dU incorporated at the cleavage site. Previous studies have shown that the additional 5-methyl group has no effect on substrate binding or chemistry [19,20].

To test for interference at A207 in the context of a ribose at the cleavage site, the four semisynthetic L-21 G414 RNAs (100 nM) were preincubated at 50°C in 10 µl of 50 mM MES, pH 5.0, 3 mM $MgCl_2$, and 1 mM $Mn(OAc)_2$ for 10 min. The RNA solutions were combined with an equal volume of radiolabeled r1d45S (~10 nM) dissolved in the same buffer, incubated for 2 min and quenched by the addition of two volumes of stop solution (8 M urea, 20 mM EDTA, pH 8.0, 0.01% xylene cyanol, 0.01% bromophenol blue). The reactions were split in half, and 100 mM iodine in ethanol (1/10 volume) was added to one portion of each reaction. The other portion was left untreated to control for background degradation of the RNA. All the RNAs were heated to 90°C for 1 min and the cleavage products resolved by 5% denaturing PAGE.

Interference suppression at A207 resulting from a 2′-deoxyribose substitution at the cleavage site was investigated by performing the reactions in 50 mM HEPES pH 7.0, 3 mM $MgCl_2$ and 1 mM $Mn(OAc)_2$ with the oligonucleotide substrate d145S, which contains a 2′-deoxyribose substitution at the cleavage site. The d145S substrate reacts significantly slower than r1d45S, which necessitates using higher pH and longer reaction times to reach a comparable level of reactivity. The ribozymes were preincubated at 50°C for 10 min, combined with the substrate and incubated at 50°C for 60 min. The reactions were treated with iodine as described above. The gels from both experiments were dried and the intensity of the cleavage products quantitated by PhosphorImager analysis. The extent of analog incorporation at each position in the transcript was obtained by 5′-end-labeling the original unselected RNA transcripts with γ-^{32}P-ATP and T4 polynucleotide kinase [59]. The 5′-end-labeled RNAs were cleaved with iodine and the cleavage products resolved by PAGE.

Figure 10

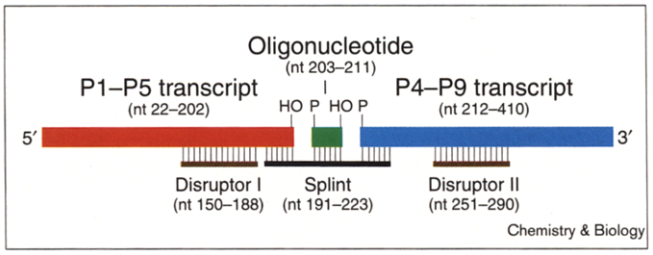

Semisynthetic preparation of A207-substituted ribozymes using T4 DNA ligase and a DNA splint.

The 5′-end-labeled control and the 3′-end-labeled selected RNAs were used to calculate the magnitude of ^{F}AαS interference at each position (Figure 6b) by substituting individual band intensities into the equation:

$$\frac{\text{AαS 3′ – Ligation reaction}}{{}^{F}\text{AαS 3′ – Ligation reaction}} \Big/ \frac{\text{AαS 5′ – Labeled control}}{{}^{F}\text{αA 5′ – Labeled control}} \qquad (1)$$

The resulting value normalizes for phosphorothioate effects and variability in the extent of analog incorporation at each position. All the interference values within two standard deviations of the mean were then averaged (the averages ranged from 0.8 to 1.2) and the result divided into the individual interference values to normalize the data for differences in loading and extent of reaction between lanes. In this calculation a value of 1 indicates no interference, whereas a value greater than 2 indicates significant interference caused by analog substitution at the specific site.

Preparation of the A207-substituted ribozymes

Full-length L-21 ScaI ribozymes containing specific nucleotide substitutions at A207 were prepared semi-synthetically by ligation of three RNA fragments, two T7 RNA polymerase transcripts (termed P1–P5 and P4–P9) and a nine-base synthetic oligonucleotide (Figure 10). The 5′-fragment (P1–P5) corresponding to positions 22–202 was transcribed from the plasmid pUCP1–P5SunY as an RNA fusion with a modified version of the SunY ribozyme at its 3′-end [63]. Plasmid pUCP1-P5SunY was prepared by PCR amplification from the plasmids pUCL-21G414 and pSC931 followed by subcloning of the full length PCR product into the *EcoRI* and *HindIII* sites of pUC19. The internal guide sequence of the SunY ribozyme was modified to be complementary to nucleotides 197–202 from P1-P5 and to cleave after U202. Processing of the P1-P5SunY fusion provided a P1–P5 RNA with a uniform 3′ terminus and a free 3′-OH due to post-transcriptional RNA processing.

P1–P5 was transcribed from *EarI* cut pUCP1–P5SunY (200 µg) at 37°C for 90 min in transcription buffer containing 20 mM $MgCl_2$, 40 mM Tris–HCl, pH 7.5, 4 mM spermidine, 0.05% Triton X-100, 4 mM each NTP, 40 units inorganic pyrophosphatase (Sigma), and 15,000 units T7 RNA polymerase. The reaction was incubated at 50°C for an additional 60 min to promote processing of the SunY intron from P1–P5. The reaction was phenol/chloroform extracted, ethanol precipitated, resuspended in TE and the products resolved by PAGE (6% acrylamide, 7 M urea). The P1–P5 fragment was cut from the gel, eluted into TE, ethanol precipitated, and redissolved in TE. In the course of the transcription incubations about 70% of the P1–P5SunY fusion RNA processed to yield P1–P5. The transcription reaction yielded about 2 nmoles of purified RNA/ml transcription.

The 3′-half of the intron (P4–P9), corresponding to positions 212–410, was transcribed from *ScaI* cut plasmid pUCP4-P9, which was prepared

by PCR amplification, followed by cloning into the *EcoR*I and *Hind*III sites of pUC19 to create a DNA template with the T7 promoter adjacent to intron position G212. P4–P9 RNA was transcribed at 37°C for 120 min in a reaction containing 15 mM $MgCl_2$, 40 mM Tris–HCl, pH 7.5, 4 mM spermidine, 0.05% Triton X-100, 2 mM each NTP, 50 units inorganic pyrophosphatase, 25,000 units T7 RNA polymerase, and 20 mM GMP to incorporate a 5′-phosphate for use in ligation. The RNA was purified as described for P1–P5, yielding about 3 nmoles of purified RNA/ml transcription. The three 9-mer synthetic oligonucleotides (5′-CCUAAC-CAC-3′) corresponding to positions 203–211 were 5′-phosphorylated with ATP using PNK to provide a 5′-phosphate for ligation.

The P1–P5 (4 nmoles), P4–P9 (4 nmoles) and the 9-mer oligonucleotide (8 nmoles) were mixed with 4 nmoles of a 33-nt DNA splint (complementary to positions 191–223) and two DNA disruptor oligonucleotides [complementary to positions 251–290 (8 nmoles) and 150–188 (8 nmoles)] in a 400 µl reaction containing 25 mM Tris–HCl, pH 7.0 and 25 mM NaCl (Figure 10). The RNA and DNA segments were annealed by heating to 90°C for 2 min and cooling the reaction slowly to room temperature. The ligation reaction was initiated by the addition of ATP (0.5 mM), fresh DTT (4 mM), 50 mM Tris–HCl, pH 7.5, 10 mM $MgCl_2$, and 800 Weiss units of T4 DNA ligase in a final reaction volume of 600 µl. The ligation reactions were incubated at 25°C for 4 h, phenol–chloroform extracted, ethanol precipitated. The full-length L-21 ScaI RNAs were purified using PAGE (6% acrylamide, 7 M urea) and concentrated as described for the P1–P5 RNA.

Although ligation of the P4–P9 fragment to the 9-mer oligonucleotide was reasonably efficient (50%), ligation of the P1–P5 fragment to the oligonucleotide proceeded very inefficiently (5% yield). The overall ligation efficiency for the full-length material was about 2%. This significantly limited the number of experiments that could be performed with the A207 substituted ribozymes, though it was possible to generate a sufficient amount of material for the basic characterizations described above. A total of three RNAs were prepared in this manner. rA207 contained a ribose at A207 and was chemically equivalent to the wild-type L-21 ScaI RNA. dA207 and ^{F}A207 contained a single 2′-deoxynucleotide or 2′-deoxy-2′-flouronucleotide substitution at A207, respectively.

Thermodynamic and kinetic characterization of A207-substituted ribozymes

Equilibrium dissociation constants (K_d) for the ribozyme 5′-exon complex were measured at 40°C using native gel mobility shift analysis under conditions of excess ribozyme and a trace concentration ($\leq K_d/10$) of 5′-^{32}P-labeled 5′-exon analog r1P (GGCCCUCrT) or d1P (CCCUCdT) [64]. Each ribozyme was prefolded at 50°C for 20 min in 50 mM Tris–HCl (pH 7.5), 10 mM NaCl, 0.1 mM EDTA, 4 mM $MgCl_2$. The solution was cooled to 40°C and combined with an equal volume of the 5′-exon oligonucleotide analog dissolved in the same buffer plus 6% glycerol and 0.1% xylene cyanol. The solution was incubated for 30 min at 40°C and the bound and free 5′-exon analog fractions separated by PAGE (8% acrylamide, nondenaturing, 4 mM $MgCl_2$, 100 mM Tris–HEPES pH 7.5). The fraction of oligonucleotide bound (θ) at each ribozyme concentration, [E], was quantitated by PhosphorImager analysis. The K_d was calculated by the nonlinear least squares fit of the equation $\theta = [E]/([E] + K_d)$. The values reported in Table 1 are an average of at least three independent experimental trials.

Measurement of $(k_{cat}/K_m)^G$, k_{cat}, and $K_m{}^G$ for the single turnover cleavage of the oligonucleotide substrates r1S (GGCCCUCrTAAAAA) or d1S (CCCUCdTAAAAA) by the L-21 ScaI form of the *Tetrahymena* ribozyme followed previously described methods [8,20,43,44]. The transcribed L-21 ScaI RNA or its A207 substituted variants were incubated in reaction buffer (50 nM ribozyme, 50 mM HEPES pH 7.0, 10 mM $MgCl_2$) at 50°C for 20 min, cooled to 30°C, and the reaction was initiated by the addition of an equal volume of the same buffered solution containing 5′-^{32}P-labeled oligonucleotide (<1 nM) and GMP (1 µM to 5 mM), prewarmed to 30°C. Portions of the reaction were removed at various times and quenched on ice with 2 volumes of 7.5 M urea, 20 mM EDTA, 0.1% xylene cyanol, 0.1% bromophenol blue. Reaction products were resolved from the unreacted substrate by denaturing 20% PAGE. The fraction reacted at each time point measured by PhosphorImager analysis, and the reaction rate (k_{obs}) at each GMP concentration was calculated using an exponential decay with an endpoint. $(k_{cat}/K_m)^G$ at low GMP concentration was calculated as a linear fit to the plot of k_{obs} verses GMP concentration [8]. The rate constants k_{cat} and $K_m{}^G$ for each enzyme were calculated by plotting k_{obs} versus GMP concentration and fitting to the equation $k_{obs} = k_{cat}[GMP]/(K_m{}^G + [GMP])$ [44]. The values reported in Table 2 are the combination of at least three independent experimental trials. No increase in k_{obs} was observed upon doubling the ribozyme concentrations at saturating GMP concentration.

Acknowledgements

We thank R. Sousa for the clone of the Y639F mutant T7 RNA polymerase, B. Ross of Isis Pharmaceuticals Inc. for the gift of 2′-deoxy-2′ fluoroadenosine, both as a nucleoside and as a protected phosphoramidite, J. Doudna for plasmid pSC931, and A. Szewczak for assistance with molecular modeling. We also thank members of the Strobel lab for critical comments on the manuscript. This work was supported by NIH grant GM54839, a Beckman Young Investigator Award, and a Searle Scholar award. S.A.S. is supported by a Junior Faculty Research Award from the American Cancer Society.

References

1. Narlikar, G.J. & Herschlag, D. (1997). Mechanistic aspects of enzymatic catalysis: lessons from comparison of RNA and protein enzymes. *Annu. Rev. Biochem.* **66**, 19-59.
2. Strater, N., Lipscomb, W.N., Klabunde, T. & Krebs, B. (1996). Two-metal ion catalysis in enzymatic acyl- and phosphoryl-transfer reactions. *Angew. Chem. Int. Ed. Engl.* **35**, 2024-2055.
3. Cech, T.R. (1990). Self-splicing of group I introns. *Ann. Rev. Biochem.* **59**, 543-568.
4. Cech, T.R. (1987). The chemistry of self-splicing RNA and RNA enzymes. *Science* **236**, 1532-1539.
5. Been, M.D. & Perrotta, A.T. (1991). Group I intron self-splicing with adenosine: evidence for a single nucleoside-binding site. *Science* **252**, 434-438.
6. Zaug, A.J., Grosshans, C.A. & Cech, T.R. (1988). Sequence-specific endoribonuclease activity of the *Tetrahymena* ribozyme: enhanced cleavage of certain oligonucleotide substrates that form mismatched ribozyme-substrate complexes. *Biochemistry* **27**, 8924-8931.
7. Beaudry, A.A. & Joyce, G.F. (1992). Directed evolution of an RNA enzyme. *Science* **257**, 635-641.
8. Herschlag, D. & Cech, T.R. (1990). Catalysis of RNA cleavage by the *Tetrahymena thermophila* ribozyme. 1. Kinetic description of the reaction of an RNA substrate complementary to the active site. *Biochemistry* **29**, 10159-10171.
9. Mei, R. & Herschlag, D. (1996). Mechanistic investigations of a ribozyme derived from the *Tetrahymena* group I intron. Insights into catalysis and the second step of self-splicing. *Biochemistry* **35**, 5796-5809.
10. Bevilacqua, P.C., Kierzek, R., Johnson, K.A. & Turner, D.H. (1992). Dynamics of ribozyme binding of substrate revealed by fluorescence-detected stopped-flow methods. *Science* **258**, 1355-1358.
11. Herschlag, D. (1992). Evidence for processivity and two-step binding of the RNA substrate from studies of J1/2 mutants of the *Tetrahymena* ribozyme. *Biochemistry* **31**, 1386-1399.
12. Bass, B.L. & Cech, T.R. (1984). Specific interaction between the self-splicing RNA of *Tetrahymena* and its guanosine substrate: implications for biological catalysis by RNA. *Nature* **308**, 820-826.
13. Moran, S., Kierzek, R. & Turner, D.H. (1993). Binding of guanosine and 3′ splice site analogues to a group I ribozyme: interactions with functional groups of guanosine and with additional nucleotides. *Biochemistry* **32**, 5247-5256.
14. Li, Y. & Turner, D.H. (1997). Effects of Mg^{2+} and the 2′-OH of guanosine on steps required for substrate binding and reactivity with the *Tetrahymena* ribozyme reveal several local folding transitions. *Biochemistry* **36**, 11131-11139.
15. Herschlag, D. & Cech, T.R. (1990). DNA cleavage catalysed by the ribozyme from *Tetrahymena*. *Nature* **344**, 405-409.
16. Herschlag, D., Eckstein, F. & Cech, T.R. (1993). The importance of being ribose at the cleavage site in the *Tetrahymena* ribozyme reaction. *Biochemistry* **32**, 8312-8321.

17. Herschlag, D., Eckstein, F. & Cech, T.R. (1993). Contributions of 2'-hydroxyl groups of the RNA substrate to binding and catalysis by the *Tetrahymena* ribozyme. An energetic picture of an active site composed of RNA. *Biochemistry* **32**, 8299-8311.
18. Knitt, D.S., Narlikar, G.J. & Herschlag, D. (1994). Dissection of the role of the conserved G·U pair in group I RNA self-splicing. *Biochemistry* **33**, 13864-13879.
19. Strobel, S.A. & Cech, T.R. (1995). Minor groove recognition of the conserved G·U pair at the *Tetrahymena* ribozyme reaction site. *Science* **267**, 675-679.
20. Strobel, S.A. & Cech, T.R. (1996). Exocyclic amine of the conserved G·U pair at the cleavage site of the *Tetrahymena* ribozyme contributes to 5'-splice site selection and transition state stabilization. *Biochemistry* **35**, 1201-1211.
21. Narlikar, G.J., Khosla, M., Usman, N. & Herschlag, D. (1997). Quantitating tertiary binding energies of 2'-OH groups on the P1 duplex of the *Tetrahymena* ribozyme: Intrinsic binding energy in an RNA enzyme. *Biochemistry* **36**, 2465-2477.
22. Pyle, A.M. (1993). Ribozymes: a distinct class of metalloenzymes. *Science* **261**, 709-714.
23. Grosshans, C.A. & Cech, T.R. (1989). Metal ion requirements for sequence-specific endoribonuclease activity of the *Tetrahymena* ribozyme. *Biochemistry* **28**, 6888-6894.
24. Piccirilli, J.A., Vyle, J.S., Caruthers, M.H. & Cech, T.R. (1993). Metal ion catalysis in the *Tetrahymena* ribozyme reaction. *Nature* **362**, 85-88.
25. Weinstein, L.B., Jones, B.C.N.M., Cosstick, R. & Cech, T.R. (1997). A second catalytic metal ion in a group I ribozyme. *Nature* **388**, 805-808.
26. Sjoegren, A.S., Pettersson, E., Sjoeberg, B.M. & Stroemberg, R. (1997). Metal ion interaction with cosubstrate in self-splicing of group I introns. *Nucleic Acids Res.* **25**, 648-653.
27. Pyle, A.M. & Cech, T.R. (1991). Ribozyme recognition of RNA by tertiary interactions with specific ribose 2'-OH groups. *Nature* **350**, 628-631.
28. Bevilacqua, P.C. & Turner, D.H. (1991). Comparison of binding of mixed ribose-deoxyribose analogues of CUCU to a ribozyme and to GGAGAA by equilibrium dialysis: evidence for ribozyme specific interactions with 2' OH groups. *Biochemistry* **30**, 10632-10640.
29. Herschlag, D., Eckstein, F. & Cech, T.R. (1993). Contributions of 2'-hydroxyl groups of the RNA substrate to binding and catalysis by the *Tetrahymena* ribozyme. An energetic picture of an active site composed of RNA. *Biochemistry* **32**, 8299-8311.
30. Strobel, S.A. & Cech, T.R. (1993). Tertiary interactions with the internal guide sequence mediate docking of the P1 helix into the catalytic core of the *Tetrahymena* ribozyme. *Biochemistry* **32**, 13593-13604.
31. Narlikar, G.J., Gopalakrishnan, V., McConnell, T.S., Usman, N. & Herschlag, D. (1995). Use of binding energy by an RNA enzyme for catalysis by positioning and substrate destabilization. *Proc. Natl Acad. Sci. USA* **92**, 3668-3672.
32. Holbrook, S.R., Cheong, C., Tinoco, I. & Kim, S.-H. (1991). Crystal structure of an RNA double helix incorporating a track of non-Watson–Crick base pairs. *Nature* **353**, 579-581.
33. Strobel, S.A., Ortoleva-Donnelly, L., Ryder, S.P., Cate, J.H. & Moncoeur, E. (1998). Complementary sets of noncanonical base pairs mediate RNA helix packing in the group I intron active site. *Nat. Struct. Biol.* **5**, 60-66.
34. Gaur, R.K. & Krupp, G. (1993). Modification interference approach to detect ribose moieties important for the optimal activity of a ribozyme. *Nucleic Acids Res.* **21**, 21-26.
35. Strobel, S.A. & Shetty, K. (1997). Defining the chemical groups essential for *Tetrahymena* group I intron function by nucleotide analog interference mapping. *Proc. Natl Acad. Sci. USA* **94**, 2903-2908.
36. Gish, G. & Eckstein, F. (1988). DNA and RNA sequence determination based on phosphorothioate chemistry. *Science* **240**, 1520-1522.
37. Young, B., Herschlag, D. & Cech, T.R. (1991). Mutations in a nonconserved sequence of the *Tetrahymena* ribozyme increase activity and specificity. *Cell* **67**, 1007-1019.
38. Moore, M.J. & Sharp, P.A. (1992). Site-specific modification of pre-mRNA: the 2'-hydroxyl groups at the splice sites. *Science* **256**, 992-997.
39. Szewczak, A.A., Ortoleva-Donnelly, L., Ryder, S.P., Moncouer, E. & Strobel, S.A. (1998). A minor groove triple helix in the active site of the *Tetrahymena* group I intron. *Nat. Struct. Biol.* **5**, 1037-1042.
40. Strobel, S.A. & Cech, T.R. (1994). Translocation of an RNA duplex on a ribozyme. *Nat. Struct. Biol.* **1**, 13-17.
41. Ortoleva-Donnelly, L., Kronman, M. & Strobel, S.A. (1998). Identifying sites of RNA tertiary structure by Nucleotide Analog Interference Mapping with N^2-methylguanosine. *Biochemistry* **37**, 12933-12942.
42. Pyle, A.M., McSwiggen, J.A. & Cech, T.R. (1990). Direct measurement of oligonucleotide substrate binding to wild-type and mutant ribozymes from *Tetrahymena*. *Proc. Natl Acad. Sci. USA* **87**, 8187-8191.
43. Herschlag, D., Piccirilli, J.A. & Cech, T.R. (1991). Ribozyme-catalyzed and nonenzymatic reactions of phosphate diesters: rate effects upon substitution of sulfur for a nonbridging phosphoryl oxygen atom. *Biochemistry* **30**, 4844-4854.
44. McConnell, T.S., Cech, T.R. & Herschlag, D. (1993). Guanosine binding to the *Tetrahymena* ribozyme: thermodynamic coupling with oligonucleotide binding. *Proc. Natl Acad. Sci. USA* **90**, 8362-8366.
45. Damberger, S.H. & Gutell, R.R. (1994). A comparative database of group I intron structures. *Nucleic Acids Res.* **22**, 3508-3510.
46. Cate, J.H., *et al.*, & Doudna, J.A. (1996). Crystal structure of a group I ribozyme domain: principles of RNA packing. *Science* **273**, 1678-1685.
47. Cech, T.R., Herschlag, D., Piccirilli, J.A. & Pyle, A.M. (1992). RNA catalysis by a group I ribozyme. *J. Biol. Chem.* **267**, 17479-17482.
48. Bass, B.L. & Cech, T.R. (1986). Ribozyme inhibitors: deoxyguanosine and dideoxyguanosine are competitive inhibitors of self-splicing of the *Tetrahymena* ribosomal ribonucleic acid precursor. *Biochemistry* **25**, 4473-4477.
49. Lienhard, G.E. (1973). Enzymatic catalysis and transition-state theory. *Science* **180**, 149-180.
50. Jencks, W.P. (1975). Binding energy, specificity, and enzymic catalysis: the Circe effect. *Adv. Enzymol.* **43**, 219-410.
51. Narlikar, G.J., Gopalakrishnan, V., McConnell, T.S., Usman, N. & Herschlag, D. (1995). Use of binding energy by an RNA enzyme for catalysis by positioning and substrate destabilization. *Proc. Natl Acad. Sci. USA* **92**, 3668-3672.
52. Narlikar, G.J. & Herschlag, D. (1998). Direct demonstration of the catalytic role of binding interaction in an enzymatic reaction. *Biochemistry* **37**, 9902-9911.
53. Steitz, T.A. & Steitz, J.A. (1993). A general two-metal-ion mechanism for catalytic RNA. *Proc. Natl Acad. Sci. USA* **90**, 6498-6502.
54. Beese, L.S. & Steitz, T.A. (1991). Structural basis for the 3'–5' exonuclease activity of *Escherichia coli* DNA polymerase I: a two metal ion mechanism. *EMBO J.* **10**, 25-33.
55. Derbyshire, V., Grindley, N.D.F. & Joyce, C.M. (1991). The 3'–5' exonuclease of DNA polymerase I of *Escherichia coli*: contribution of each amino acid at the active site to the reaction. *EMBO J.* **10**, 17-24.
56. Zhang, Y., Liang, J.-Y., Huang, S., Ke, H. & Lipscomb, W.N. (1993). Crystallographic studies of the catalytic mechanism of the neutral form of fructose-1,6-bisphosphatase. *Biochemistry* **32**, 1844-1857.
57. Marcus, C.J. (1976). Inhibition of bovine hepatic fructose-1,6-diphosphatase by substrate analogs. *J. Biol. Chem.* **251**, 2963.
58. El-Maghrabi, M.R., Gidh-Jain, M., Austin, L.R. & Pilkis, S.J. (1993). Isolation of a human liver fructose-1,6-bisphosphatase cDNA and expression of the protein in *Escherichia coli*. Role of Asp-118 and Asp-121 in catalysis. *J. Biol. Chem.* **268**, 9466-9472.
59. Ortoleva-Donnelly, L., Szewczak, A.A., Gutell, R.R. & Strobel, S.A. (1998). The chemical basis of adenosine conservation throughout the *Tetrahymena* ribozyme. *RNA* **4**, 498-519.
60. Scaringe, S.A., Wincott, F.E. & Caruthers, M.H. (1998). Novel RNA synthesis method using 5'-O-silyl-2'-O-orthoester protecting groups. *J. Am. Chem. Soc.* **120**, 11820-11821.
61. Sousa, R. & Padilla, R. (1995). A mutant T7 RNA polymerase as a DNA polymerase. *EMBO J.* **14**, 4609-4621.
62. Lingner, J. & Keller, W. (1993). 3'-end labeling of RNA with recombinant yeast poly(A) polymerase. *Nucleic Acids Res.* **21**, 2917-2920.
63. Doudna, J.A. & Szostak, J.W. (1989). Miniribozymes, small derivatives of the *sunY* intron, are catalytically active. *Mol. Cell. Biol.* **9**, 5480-5483.
64. Pyle, A.M., Moran, S., Strobel, S.A., Chapman, T., Turner, D.H. & Cech, T.R. (1994). Replacement of the Conserved G·U with a G-C pair at the cleavage site of the *Tetrahymena* ribozyme decreases binding, reactivity, and fidelity. *Biochemistry* **33**, 13856-13863.

Because *Chemistry & Biology* operates a 'Continuous Publication System' for Research Papers, this paper has been published via the internet before being printed. The paper can be accessed from http://biomednet.com/cbiology/cmb – for further information, see the explanation on the contents pages.